From calorimetry to thermal risk assessment: γ-valerolactone production from the hydrogenation of alkyl levulinates

Yanjun Wang[1], *Igor Plazl*[2], *Lamiae Vernières-Hassimi*[1], *Sébastien Leveneur*[1]*

[1]*Normandie Univ, INSA Rouen, UNIROUEN, LSPC, EA4704, 76000 Rouen, France, E-mail : sebastien.leveneur@insa-rouen.fr*

[2]*Faculty of Chemistry and Chemical Technology, University of Ljubljana, Večna pot 113, 1000 Ljubljana, Slovenia*

Abstract.

The use of lignocellulosic biomass as a raw material can sustain the chemical industry. There is a lack of knowledge in kinetics and thermodynamics of some of these processes, making difficult the cost analysis. For instance, the thermodynamic investigation of the hydrogenation of alkyl levulinates to γ-valerolactone (GVL) is seldom. This system is a two-step reaction comprising a hydrogenation and cyclization step. The experimental measurement of the two reaction enthalpies is challenging, and a method was developed in this manuscript. The hydrogenation of methyl levulinate (ML) and butyl levulinate (BL) in the GVL solvent was found to be an exothermic step, and the cyclization an endothermic one. The reaction enthalpy for the hydrogenation of ML in the GVL solvent, calculated to -53.25 kJ/mol, is higher than the one of BL in the GVL solvent, calculated to -38.66 kJ/mol. The reaction enthalpies for the cyclization step are similar for ML and BL system, i.e., +7.00 kJ/mol and +6.50 kJ/mol, respectively. Hence, the hydrogenation step governs the reaction temperature. A thermal risk assessment based on experiments performed under adiabatic condition was done. The thermal risk was found to be medium for this reaction system under the operating conditions used in this study.

Keywords: reaction enthalpies, calorimetry, biomass valorization, thermal risk, kinetic modeling, γ-valerolactone production

Highlights

- Determination of the reaction enthalpy of the first and second steps for the hydrogenation of methyl and n-butyl levulinates.
- Development of kinetic models for the hydrogenation of methyl and n-butyl levulinates over Ru/C catalyst under adiabatic conditions.
- The thermal risk was evaluated to be medium for the hydrogenation of methyl and n-butyl levulinates.

1. INTRODUCTION

The use of biomass as a raw material for the production of chemicals, fuels and materials can be seen as a game-changer in the chemical industry. From an environmental viewpoint, these raw materials are more ecofriendly than fossil raw materials because they are renewable. From a societal and political viewpoint, the use of local biomass could revitalize rural areas and create new jobs (Budzianowski and Postawa, 2016).

The choice of biomass raw material is crucial and must respect several criteria, such as:

- The cultivation of this biomass should not lead to soil and groundwater pollution.
- The biomass should not be used in the alimentary sector.
- An optimum synergy between the harvest, transportation and storage should be found.
- A total valorization of the biomass must be done.

In order to avoid the dilemma of food versus fuel, the use of second-generation biomass as a raw material in the chemical industry should be privileged. Second-generation biomass can be lignocellulosic biomass, agricultural waste, or dedicated non-food crops (miscanthus, switchgrass) on non-agricultural lands.

The valorization of lignocellulosic biomass at the industrial scale has considerably increased these recent years (Chandel et al., 2020). One of the main challenges is the pretreatment step to separate lignin, cellulose, and hemicellulose for further upgrading into valuable chemicals, fuels, or materials. One can mention the commercial-scale cellulosic ethanol production plant by GranBio company in Brazil, with a capacity production of 82 million liters per year (GranBio, 2014). Energy cane, straw and sugarcane bagasse can be used as raw materials. These raw materials were

pretreated by steam explosion, and then enzymatic processes were used for hydrolysis and fermentation steps. Another successful lignocellulosic industrial application is the Borregaad plant in Sarpsborg (Norway), producing vanillin via the sulfite pulping method (Wong, 2012). This plant has a production capacity of 250 tonnes per year and used spruce trees as feedstocks (Borregaard, 2019).

Another promising molecule produced from lignocellulosic biomass and more specifically from cellulose and hemicellulose is levulinic acid, which was classified as a top 10 building blocks or platform molecules by the U.S. Department of Energy (Gallezot, 2012). Levulinic acid is industrially produced from the acid hydrolysis of cellulose (Hayes et al., 2005). At the industrial scale, GFBiochemicals is the main company to produce this molecule (ca. 10000 tonnes per year) via ATLAS Technology^{TM} (Makhubela and Darkwa, 2018; Pulidindi and Kim, 2020). There is also a growing interest to study the production of alkyl levulinates from the alcoholysis of cellulose or hemicellulose (Peng et al., 2011; Wu et al., 2012; Ding et al., 2015; An et al., 2017; Di Bitonto et al., 2018). These levulinates are still considered as platform molecules with the primary benefits to be less corrosive than levulinic acid.

Further upgrading of levulinic acid or alkyl levulinates is by hydrogenation to γ-valerolactone (GVL). This molecule is of particular interest because it is also a platform molecule (Yan et al., 2015). Indeed, GVL can be used as fuel additives and solvents and has excellent potential for further upgrading to valuable chemicals, materials, and fuels (Bozell et al., 2000; Huber et al., 2006; Horváth et al., 2008; Bond et al., 2010; Serrano-Ruiz et al., 2010; Alonso et al., 2012; Qi and Horváth, 2012; Wettstein et al., 2012; Luterbacher et al., 2014; Mellmer et al., 2014; Tukacs et al., 2015; Rodenas et al., 2018; Sener et al., 2018; Al-Naji et al., 2019)

The use of molecular hydrogen to produce this molecule from LA or alkyl levulinates is widely studied by different research groups to find the best catalyst (Wright and Palkovits, 2012; Luo et al., 2013; Tang et al., 2014; Dutta et al., 2019; Tanwongwan et al., 2019; Wojciechowska et al., 2019; Feng et al., 2020), to intensify this process (Bourne et al., 2007; Al-Shaal et al., 2016), or to develop advanced kinetic models (Piskun et al., 2016; Negahdar et al., 2017; Li et al., 2018; Wang et al., 2019; Protsenko et al., 2020). The most common heterogeneous catalyst for this reaction is Ru/C. The hydrogenation of LA of alkyl levulinate over Ru/C to GVL is a two-step reaction (scheme 1).

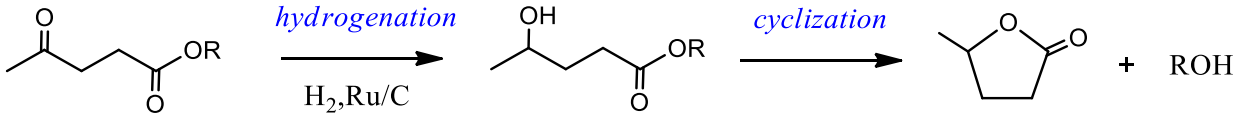

Scheme 1. Mechanism of hydrogenation of alkyl levulinates to GVL.

Few papers are dealing with the safety aspect of this reaction system (Wang et al., 2018; Casson-Moreno et al., 2019), which can be a severe issue. Indeed, the use of biomass feedstock receives a positive perception from public opinion as shown by different studies (Zoellner et al., 2008; Dockerty et al., 2012; Soland et al., 2013; Kortsch et al., 2015; Sikorska et al., 2020), except when there is a risk of air pollution (Upham and Shackley, 2007). A risk assessment must be performed to implement adequate safety barriers to preserve the excellent perception of such industries. For instance, it was shown that several accidents occurred in the bioenergy production sector (Casson-Moreno and Cozzani, 2015; Casson-Moreno et al., 2015; Brown et al., 2016).

In a previous study, it was shown that hydrogenation of levulinic acid in water solvent could present a severe risk of thermal runaway according to the operating conditions (Wang et al., 2018) The assessment of such risk must be done. Indeed, Dakkoune et al. demonstrated that this risk is responsible for around 25% of the accident in the French chemical plants (Dakkoune et al., 2018)

For quantifying a thermal risk, one needs to calculate/estimate probability and severity parameters under adiabatic conditions and in batch mode, i.e., the worst-case scenario (Stoessel, 2008; Leveneur et al., 2016). The knowledge of the Time-to-Maximum Rate under adiabatic conditions (TMR_{ad}) parameter can assess the probability of thermal runaway (Stoessel, 2008). This parameter is defined as the time to reach the maximum temperature rate. The adiabatic temperature rise under adiabatic condition (ΔT_{ad}) is a parameter evaluating the severity of the thermal risk. To estimate these thermal risk parameters at different operating conditions, one needs to investigate kinetics (reaction order, rate constants, activation energy...) and thermodynamics (specific heat capacity, reaction enthalpy…) of a chemical system.

There are several strategies to obtain these parameters. The most widespread approach is to perform some experiments in an adiabatic calorimeter and apply a zero-order approach to estimate TMR_{ad} and ΔT_{ad}. The main drawback of such an approach is that one cannot estimate the values of these parameters at different operating conditions (Vernières-Hassimi et al., 2017).

The other issue concerning the determination of these parameters comes from the experimental part. Kinetic models can be developed based on experiments performed under isothermal conditions at process temperatures, and thermodynamic constants could be measured in calorimeter or evaluated via thermodynamic models. However, this approach is not representative of a thermal runaway because one can miss the observation of secondary reactions or other side reactions occurring at higher temperatures, which could worsen the accident (Stoessel, 2008).

The thermal runaway assessment must be done based on experiments performed under adiabatic conditions. For that, there are several calorimeters: ARSST (Marco et al., 2000; Tang et al., 2009; Veedhi and Sawant, 2013; Veedhi et al., 2014; Vernières-Hassimi et al., 2017; Leveneur, 2017; Leveneur et al., 2018; Wang et al., 2018; Shen et al., 2019; Pérez-Sena et al., 2020), VPS2 (Delhaye et al., 2007; Wu et al., 2008; Chi et al., 2009; Jhu et al., 2012; Tseng et al., 2012; Liu et al., 2013; Zhang et al., 2017), PhiTecII (Singh, 1993; Sempere et al., 1997; Maestri et al., 2006; ReyesValdes et al., 2016; Saha et al., 2018; Sun et al., 2019) and RC1 (Lunghi et al., 2002; Wang et al., 2019; Wang et al., 2020). The main challenge for the gas-liquid-solid system is the mixing issue. High-pressurized RC1 Mettler-Toledo can ensure an efficient mixing for the hydrogenation of levulinic acid or alkyl levulinaves over Ru/C.

In this manuscript, thermal risk assessments of methyl levulinate and butyl levulinate hydrogenation to GVL over Ru/C were conducted. These two alkyl levulinates can be produced from the alcoholysis of cellulose and are less corrosive than GVL. The benefit of the GVL solvent is its low vapor pressure value with temperature, high flash point (96°C), and low melting point (-31°C). GVL is considered a promising solvent (Horváth et al., 2008; Lin et al., 2017; Pokorný et al., 2017; Chew et al., 2020; Liu et al., 2020). In a previous study of our group (Wang et al., 2019), it was demonstrated that hydrogenation of these alkyl levulinates in GVL over Ru/C is a two-step reaction, as illustrated by Scheme 1. Some experiments were performed in RC1 Mettler-Toledo under isothermal and adiabatic conditions. To the best of our knowledge, the use of adiabatic conditions with such reaction volume is rare in the literature.

In the first stage, a methodology was developed to experimentally measure the reaction enthalpy of each reaction step for ML and BL hydrogenation system in GVL. Two different calorimeters were used for this stage: RC1 calorimeter and Tian-Calvet calorimeter.

157 In the second stage, kinetic models for both substrates were developed based on experiments in
158 RC1 under adiabatic conditions. From the estimated kinetic constants and measured
159 thermodynamic constants, thermal risk assessment was performed.
160
161
162

2. EXPERIMENTAL SECTION

2.1 Chemicals

Methyl levulinate (wt% ⩾ 98%) and γ-valerolactone (wt% ⩾ 99%) were purchased from Sigma-Aldrich. Alfa Aesar provided n-Butyl levulinate (wt%⩾98%). Acros Organics supplied furfural (wt% ⩾ 99%). Alfa Aesar provided Ru/C (5 wt % ruthenium on activated carbon powder, reduced and 50% water wet). Linde supplied H_2 (>99.999%). Acetone (Analytical grade) was bought from VWR. Sulfuric acid (wt% ⩾ 98%) was obtained from Fisher chemicals. All the chemicals were used without further treatment.

2.2 RC1 experiments

Hydrogenation of ML or BL to GVL catalyzed over Ru/C in the GVL solvent was performed in RC1, which includes pressure system, temperature system and process control system (Fig. 1). The experiments were performed under isothermal or adiabatic, and isobaric conditions assured by the process control system and jacket temperature control system. A gas entrainment impeller was used to ensure efficient gas-liquid mixing.

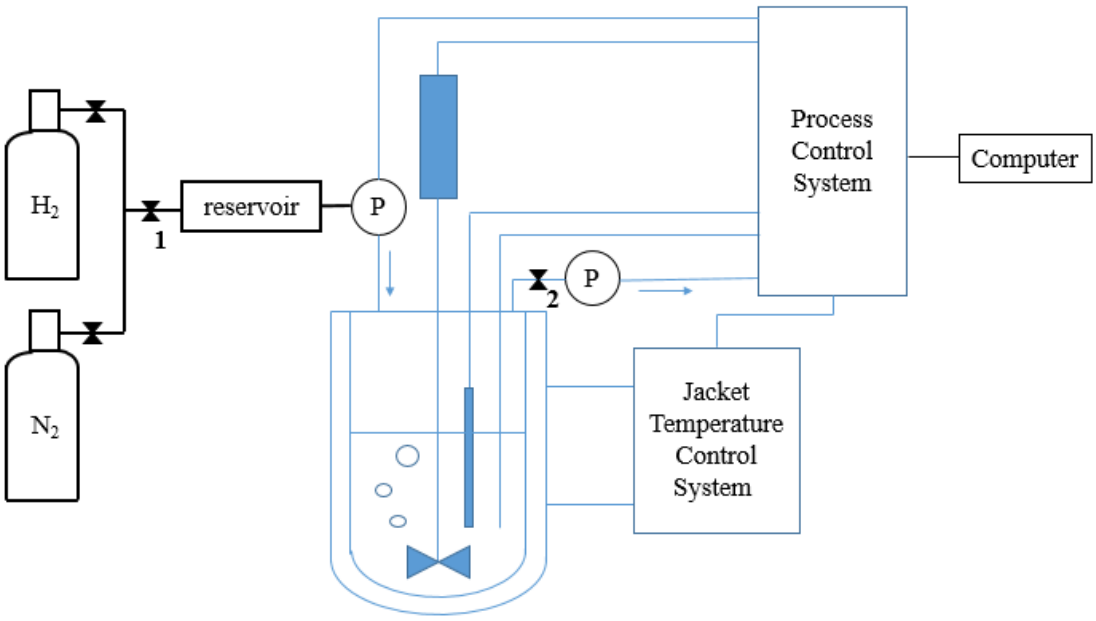

Fig. 1 - RC1 for hydrogenation of ML or BL to GVL.

2.2.1 Experiments under isothermal conditions

At first, an alkyl levulinate solution was introduced to the reactor with the Ru/C catalyst. Then, the sealed reactor was purged with nitrogen three times before increasing temperature in the reactor to 130°C. The stirring was stopped, and valve 2 was closed when the reactor temperature reached 130°C. After that, valve 1 was open, and ca. 35 bar of hydrogen was injected into the reactor. When reaching 35 bar in the reactor, valve 1 was closed, and the pressure in the reservoir was around 70 bar. In this way, the storage gas in the reservoir was enough to maintain the pressure constant in the reactor during the reaction by the automatic pressure control system. The stirring was fixed to 800 rpm to start the reaction. Under isothermal condition, the jacket temperature control system was set to keep the reaction temperature constant. During the reaction time, no sample was taken to avoid any interferences with the reaction temperature signal.

GC analyzed the initial and final reaction mixture. Table 1 shows the operating conditions for both experiments in the RC1 calorimeter.

Table 1. Operating conditions for the hydrogenation of alkyl levulinate under isothermal and isobaric conditions in RC1.

	Initial concentration (mol/L)			Catalyst loading in dry basis (kg/L)	Temperature (°C)	Pressure (Bar)
Levulinates	Substrate	GVL	Alcohol			
ML	5.15	3.90	0	5.28×10^{-3}	130	35
BL	2.04	6.79	0	5.43×10^{-3}	130	35

2.2.2 Experiments under adiabatic condition

The alkyl levulinate solution was introduced into the reactor, followed by a nitrogen purge. The initial reaction temperature was set to 100 ºC under adiabatic mode. Experiments were carried out under isobaric conditions at 35 bar. The stirring speed was set at 800 rpm to start the reaction. No samples were withdrawn during adiabatic experiments. Table 2 shows the operating conditions for both experiments in the RC1 calorimeter under adiabatic conditions.

Table 2. Operating conditions for the hydrogenation of alkyl levulinates under adiabatic and isobaric conditions in RC1.

	Initial concentration (mol/L)			Catalyst loading in dry basis (kg/L)	Initial temperature (°C)	Pressure (Bar)
	Substrate	GVL	Alcohol			
ML	4.64	3.69	0	5.42×10^{-3}	100	35
BL	4.28	1.81	0	5.43×10^{-3}	100	35

2.3 C80 experiments

Cyclization experiments were performed in the Tian-Calvet calorimeter C80 (Fig. 2) (Zheng et al., 2016). The calorimeter C80 is a differential calorimeter operating under isothermal condition and requires a small amount of reaction mixture (1g). To only measure the heat flow rate due to reaction 2, solutions with a high concentration of intermediates were prepared. For that, the RC1 calorimeter was used, and the reaction was stopped before the full conversion of the intermediate to GVL. Then, the solution was filtered to remove the heterogeneous catalyst. The solutions were stored in a fridge to quench the cyclization reaction. Table 3 shows the operating conditions for experiments in the C80.

Hastelloy cells were used: one reference cell and one measurement cell. The temperature and heat flow rate was monitored during the experiments. For this study, the experiments were performed at 60ºC to avoid liquid evaporation and cyclization reaction in the reference cell.

Table 3. Operating conditions for the ring closure experiments in C80 under isothermal conditions for the inside tube.

	Initial concentration (mol/L)			Temperature (°C)
	Substrate	GVL	Intermediate	
ML	0	7.80	1.70	60
BL	0.17	9.01	0.33	60

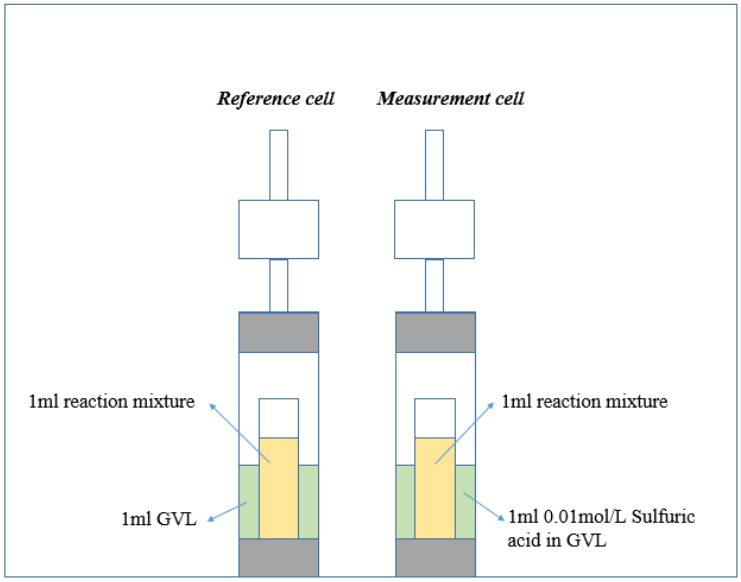

Fig. 2 - Cyclization reaction performed in C80.

The cell contains two major parts: inside an open tube and an outside container (Fig. 2). For the measurement cell, the inside tube was filled with 1 mL of the reaction mixture, and the outside was filled with 1 mL of sulfuric acid solution in GVL concentrated at 0.01 $mol.L^{-1}$. Sulfuric acid was used to catalyze the cyclization to obtain a neat signal. For the reference cell, the inside tube was filled with 1ml of the reaction mixture, and the outside container was filled with 1ml of pure GVL. The reference cell must have a similar specific heat capacity ($m \times Cp$) than the measurement one, and no reaction must occur in this cell. At this temperature and in the absence of catalyst, the cyclization kinetics is negligible. This absence of reaction in the reference cell was confirmed by GC analysis.

After the preparation of the cells, they were put inside the C80 calorimeter vertically, and the temperature of this calorimeter was fixed to 60ºC. When the temperature reached 60ºC, and the heat flow rate was stable, the calorimeter started to rotate continuously. When this rotating process started, the liquids in the inside tube and outside container were mixed, and the reaction started. After ca. 3h reaction, the rotating was stopped, and the calorimeter was cooled down. A GC analysis was carried out on the initial and final reaction mixture from the reference and measurement cells.

2.4 Analytical section

The concentration of substrates (ML, BL), intermediates (MHP, BHP), and GVL was quantified by GC-FID analysis. Samples were filtered and diluted with acetone. Furfural was used as an internal standard for quantification. Bruker Scion GC436 gas chromatography (GC) equipped with an FID detector (flame ionization detector), an autosampler, and a capillary column (Rxi-5ms, 30 m × 0.32 mm internal diameter × 0.25 μm film thickness) were used. Helium (99.99%) was used as carrier gas at a constant flow rate of 1.2 $mL.min^{-1}$. The temperature of the injector and the detector was set at 270 °C. The oven temperature was programmed as 35 °C (3 min)-15 $°C.min^{-1}$-300°C. The injection volume was 5 μL, and the split ratio was 30:1. The standard deviation of analytical measurement was found to be lower than 0.70% indicating the high repeatability of the analysis.

3. RESULTS AND DISCUSSION

3.1 Determination of reaction enthalpies

The mechanism for hydrogenation of alkyl levulinates to GVL is a two-step reaction (Scheme 1). The first step is hydrogenation of the carbonyl group to the intermediate (MHP or BHP). The second step is the cyclization of the intermediate to GVL. Based on this mechanism, one needs to evaluate/measure the two reaction enthalpies. In this study, both reaction enthalpies were calculated. GVL was used as a solvent for these experiments because BL and ML are soluble in GVL (Wang et al., 2019). The other benefit of GVL is its low vapor pressure value, e.g., 9.21×10^{-4} bar at 92.11°C, allowing to work at higher temperatures (Pokorny et al., 2017).

The reaction enthalpies $\Delta H_{R,1}$ was defined as the amount of energy released/consumed by the hydrogenation reaction per mole of alkyl levulinate consumed, and $\Delta H_{R,2}$ as the amount of energy released/consumed by the cyclization reaction per mole of GVL produced. The heat release in RC1 (Q_{RC1}) includes the heat release from step 1 (Q_1) and step 2 (Q_2) as these two steps occur consecutively. In calorimeter C80, it is possible to measure only the heat of reaction 2 in the absence of hydrogen and Ru/C catalyst. The energy equations are shown below:

$$Q_{RC1} = \int_{t=0}^{t} (-R_1 \times V \times \Delta H_1 - R_2 \times V \times \Delta H_2)\,.\,dt = Q_1 + Q_2 \quad (1)$$

$$Q_{C80} = \int_{t=0}^{t} (-R_2 \times V \times \Delta H_2)\,.\,dt = Q_2 \quad (2)$$

where, Q_1 and Q_2 represent the heat of reactions 1 and 2, respectively; R_1 and R_2 represent the reaction rates 1 and 2; ΔH_1 and ΔH_2 represent the reaction enthalpies 1 and 2, respectively.

284 Instead of measuring the reaction rates, one can consider the material balance for the substrate:

$$n_{Subs,0} = n_{Subs}(t) + n_{Int}(t) + n_{GVL}(t) - n_{GVL,0} \quad (3)$$

285 The heat release from step 1 (Q_1) depends on the first reaction enthalpy and mole conversion of
286 substrate ML or BL (Eq. 4). The heat release of Q_2 depends on the second reaction enthalpy and
287 conversion of the intermediate to GVL (Eq. 5).

$$Q_1 = -(n_{Subs,0} - n_{Subs,final}) \times \Delta H_{R,1} \quad (4)$$

$$Q_2 = +\left(n_{GVL,0} - n_{GVL,final}\right) \times \Delta H_{R,2} \quad (5)$$

288 From Eqs (1) and (2), one can obtain the equations for the calculation of reaction enthalpy:

$$\Delta H_{R,2} = \frac{+Q_{C80}}{n_{GVL,0} - n_{GVL,final}} \quad (6)$$

$$\Delta H_{R,1} = \frac{Q_{RC1} - \left(n_{GVL,0} - n_{GVL,final}\right) \times \Delta H_{R,2}}{-\left(n_{Subs,0} - n_{Subs,final}\right)} \quad (7)$$

289

290 As in C80 experiment, only step 2 occurs so the reaction enthalpy for the second step ($\Delta H_{R,2}$) can
291 be calculated firstly. Then by using the value of $\Delta H_{R,2}$, the reaction enthalpy for the first reaction
292 ($\Delta H_{R,1}$) can be obtained.

293

294 **3.1.1 RC1 results**

295 Fig. 3 shows the evolution of the heat flow rate released by the reactions for the hydrogenation of
296 ML and BL under isothermal conditions at 130°C. The time zero was set when the stirring was
297 started.

298

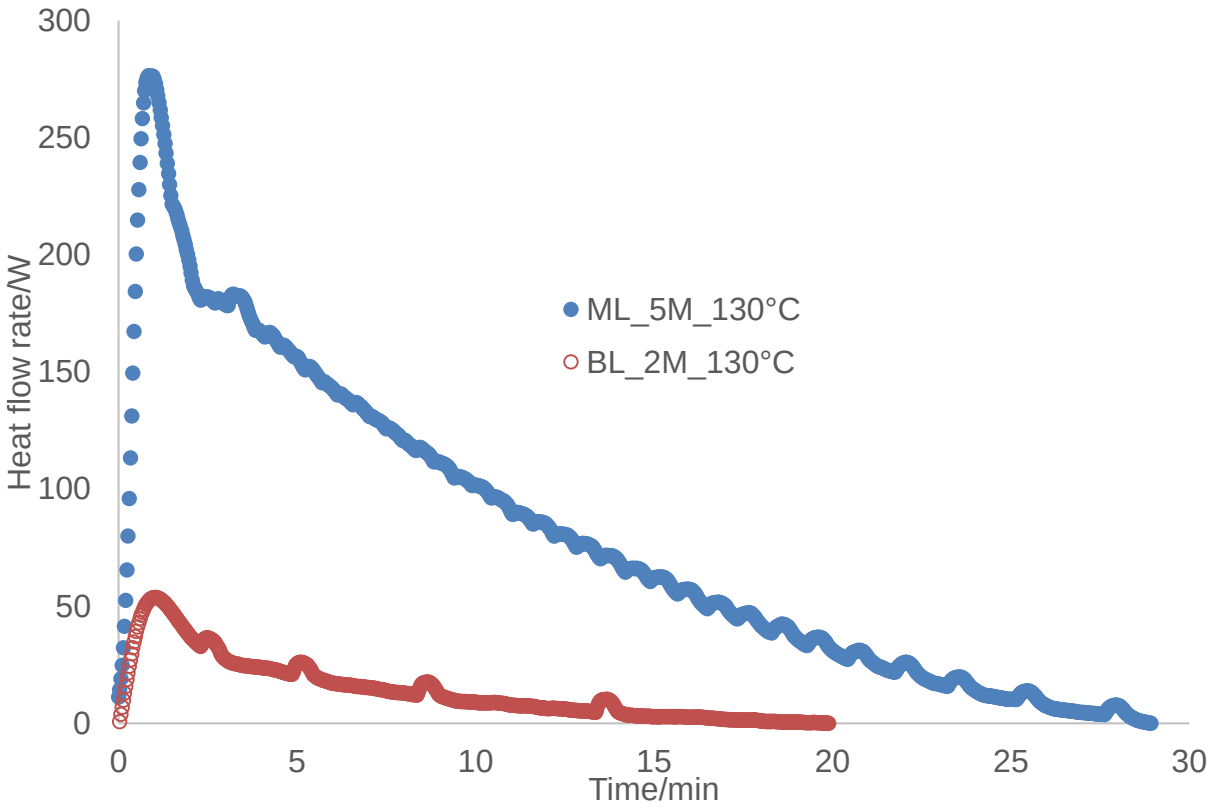

Fig. 3 - Heat flow rate for hydrogenation of ML and BL to GVL in RC1 under isothermal conditions at 130°C.

By integrating the peak area from time 0 to the end of the experiment, the total energy released (Q_{RC1}) from this reaction can be obtained (Table 4).

Table 4. GC and RC1 results for experiments under isothermal condition.

	Initial concentration (mol/L)		Final concentration (mol/L)			Q_{RC1} (kJ)
	Substrate	GVL	Substrate	GVL	Intermediate	
ML	5.15	3.9	0.00	5.16	3.40	+158.26
BL	2.04	6.79	0.44	7.26	0.79	+34.187

The reaction mixture before and after experiments were analyzed by GC (Table 4). From the material balance analysis, no side reactions were noticed. The conversion of ML was total but not the conversion of MHP to GVL. One can notice that the kinetics for the BL system was slower. Globally, these reaction systems are exothermic, and the total energy released per GVL produced by the ML system is higher than for the BL system in absolute value (Table 6).

3.1.2 C80 results

Before the C80 rotation in measurement cell, the reaction mixture in the open tube comprised substrates, intermediates, alcohols and GVL; and the outside container comprised GVL and sulfuric acid to catalyze the cyclization reaction. The time zero is when the C80 starts to rotate. The cyclization reaction is endothermic as illustrated by Fig. 4.

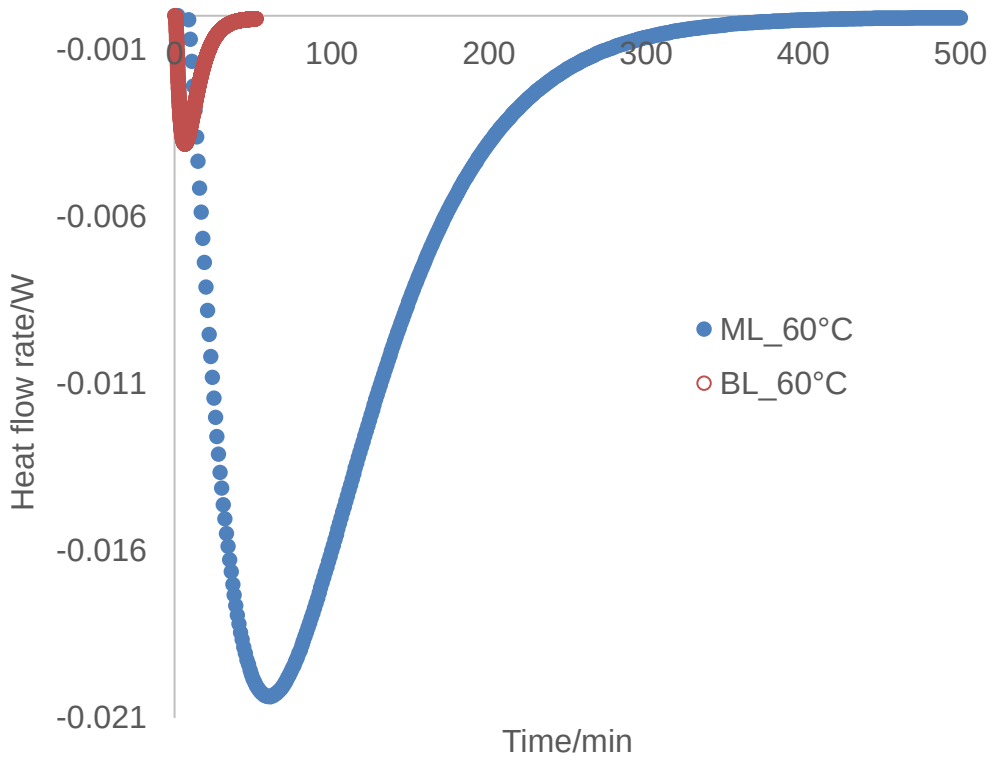

Fig. 4 - Heat flow rate profiles for the cyclization reaction of MHP and BHP in C80 at 60°C.

By integrating the heat flow rate peak, the total energy absorbed by the reaction can be calculated. Table 5 shows the results of the C80 calorimeter.

Table 5. GC and C80 experiments.

	Initial concentration (mol/L)			Final concentration (mol/L)			Q_{C80} (kJ)
	Substrate	GVL	Intermediate	Substrate	GVL	Intermediate	
ML	0.00	7.80	1.70	0.00	8.99	0.41	-0.018
BL	0.17	9.01	0.33	0.17	9.48	0.03	-0.004

From Table 5, one can notice that the energy absorbed by the second reaction is slightly higher for the MHP cyclization than for the BHP cyclization. The reaction enthalpy 2 for ML system is +7 kJ/mol, and for BL system is +6.5 kJ/mol.

From Eq. (7), one can find that the values of reaction enthalpy 1 for ML is -53.25 kJ/mol and -38.66 kJ/mol for BL. Table 6 summarizes the different reaction enthalpy.

One can conclude that reaction 1, i.e., hydrogenation, governs the reaction temperature of this system. The hydrogenation enthalpy for the ML system is higher than the one for the BL system. This observation shows that the substituent plays a role not only on the kinetics (Wang et al., 2019) but also on the thermodynamics.

Table 6. Reaction enthalpies for each step in the GVL solvent.

	ML	BL
$\Delta H_{R,1}$	-53.25 kJ/mol	-38.66 kJ/mol
$\Delta H_{R,2}$	+7.00 kJ/mol	+6.50 kJ/mol

3.2 Thermal risk assessment

The aim of this section is not to develop a detailed kinetic model based on adiabatic experiments but to calculate various thermal risk parameters such as T_{D24}, T_{D8}, $TMR_{ad}(Tp)$, and ΔT_{ad} as accurately as possible instead of the zero-order model (Vernières-Hassimi et al., 2017).

The parameter $TMR_{ad}(Tp)$ is the time to reach the maximum rate from the initial temperature Tp, and is obtained from the derivative of the reaction temperature. The parameters T_{D24} and T_{D8} are the initial temperatures to get TMR_{ad} of 24 and 8 hours, respectively. The parameter ΔT_{ad} corresponds to the difference between the final and initial temperatures. For the sake of clarity, Fig. 5 illustrates the values of these parameters.

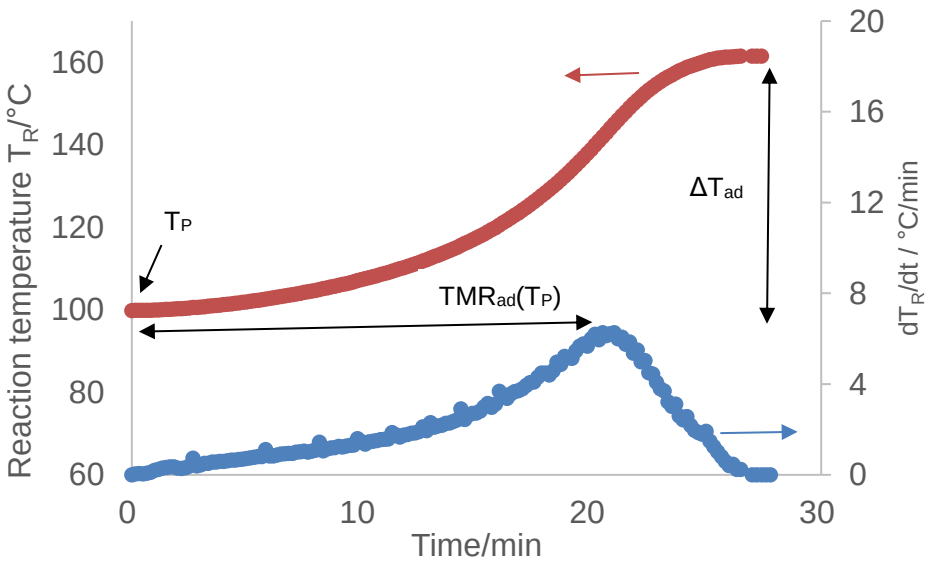

Fig. 5 – Thermal risk parameters under adiabatic conditions.

As already noted, it is the hydrogenation reaction that determines the reaction temperature, since the second enthalpy of the reaction is very low. Therefore, this second reaction can be neglected for the kinetic model under adiabatic conditions, and the reaction rate takes the following form:

$$R_1 = k_1 \times [Substrate]_{liq} \times P_{H_2} \times \omega_{Cat.} \quad (8)$$

As it was observed in the previous study of our group (Wang et al., 2019), the kinetics of hydrogen mass transfer is faster than the ones of the chemical reaction. Hence, the concentration of hydrogen in the bulk liquid phase is assumed to be the same as the one at the gas-liquid interface. The material balance equations for substrate and intermediate in the autoclave are then simply represented as:

$$\frac{d[substrate]}{dt} = -R_1 \quad (9)$$

$$\frac{d[intermediate]}{dt} = R_1 \quad (10)$$

while the heat balance equation for the liquid phase is:

$$\frac{\mathrm{d}T_R}{dt} = \frac{-R_1 \times \Delta H_{R1} \times V}{m_R \times C_{PR} + m_{insert} \times Cp_{insert}} \quad (11)$$

The term $m_R \times C_{PR}$ was evaluated by $m_R \times \left(w_{subs,0} \times Cp_{subs}(\mathrm{T}_R) + w_{GVL,0} \times Cp_{GVL}(\mathrm{T}_R)\right)$, where $w_{subs,0}$ and $w_{GVL,0}$ are the initial mass fraction of the substrates and GVL. The variation of the specific heat capacity with temperature was taken into account. According to the manufacturer, the term heat capacity of the insert is 52 J/K.

A modified Arrhenius equation was used to decrease the correlation between the pre-exponential factor and activation energy:

$$k_1(T) = k_1(T_{Ref}) \times exp\left(\frac{-Ea}{R} \times \left(\frac{1}{T} - \frac{1}{T_{Ref}}\right)\right) \quad (12)$$

As mentioned, reaction temperatures and the hydrogen pressures in the autoclave were monitored online during the hydrogenation process.

Based on the standard least-squares method, the predictions of developed model equations (Eqs 8-12) with appropriate boundary conditions were then fitted to the online measured reaction temperature, where the rate constants at a reference temperature (T_{ref}) and activation energies served as fitting parameters.

The software ModEst was used to estimate the kinetic constant of the first reaction for the ML and BL system (Haario, 1994). ODESSA, which uses the backward difference method, solved the ordinary differential equations. A Levenberg-Marquardt algorithm was used to optimize the objective function, defined as

$$\omega = \sum_i (y_i - \hat{y}_i)^2 \quad (13)$$

where, y_i is the experimental reaction temperature value and $\hat{y}_i$ is the simulated one.

Fig. 6 shows the fit of the model to the experimental temperature. One can conclude that the model can predict the temperature evolution. Table 7 displays the values of the estimated parameters and the standard deviation. The values of the standard deviation are very low. However, there is a strong correlation between the rate constant at 130°C and the activation energy, i.e., 0.992. This strong correlation might be due to the simplified kinetic model used.

Table 7. Estimated kinetic constants and standard deviation at T_{Ref}=130°C for the ML system.

	Units	Estimated parameters	Relative standard deviation (%)
$k_1(T_{Ref})$	L/(bar.kg_dry basis_cat.s)	0.535×10^{-08}	0.7
Ea_1	J/mol	$0.822\times10^{+05}$	0.6

The coefficient of determination was found to be equal to 98.92% for the modeling of BL hydrogenation under adiabatic mode. Fig. 6 shows the fit of the model to the experimental temperature. One can conclude that the model can predict the temperature evolution. Table 8 displays the values of the estimated parameters and the standard deviation. The values of the standard deviation are very low. However, there is a strong correlation between the rate constant at 130°C and the activation energy, i.e., 0.998.

Table 8. Estimated kinetic constants and standard deviation at T_{Ref}=130°C for the BL system.

	Units	Estimated parameters	Relative standard deviation (%)
$k_1(T_{Ref})$	L/(bar.kg_dry basis_cat.s)	0.350×10^{-08}	2.3
Ea_1	J/mol	$0.857\times10^{+05}$	1.3

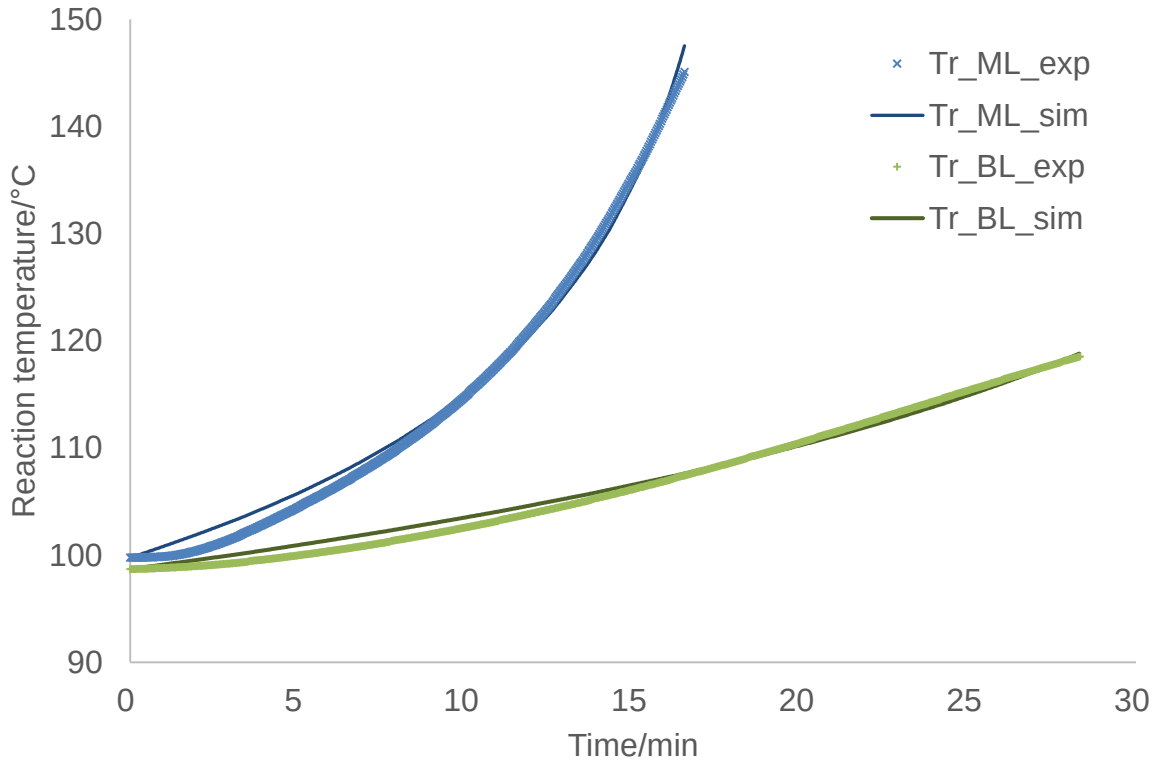

407

408 Fig. 6 - Temperature profiles for the hydrogenation of BL and ML under adiabatic conditions.

409 Figs 7 show the high reliability of both models.

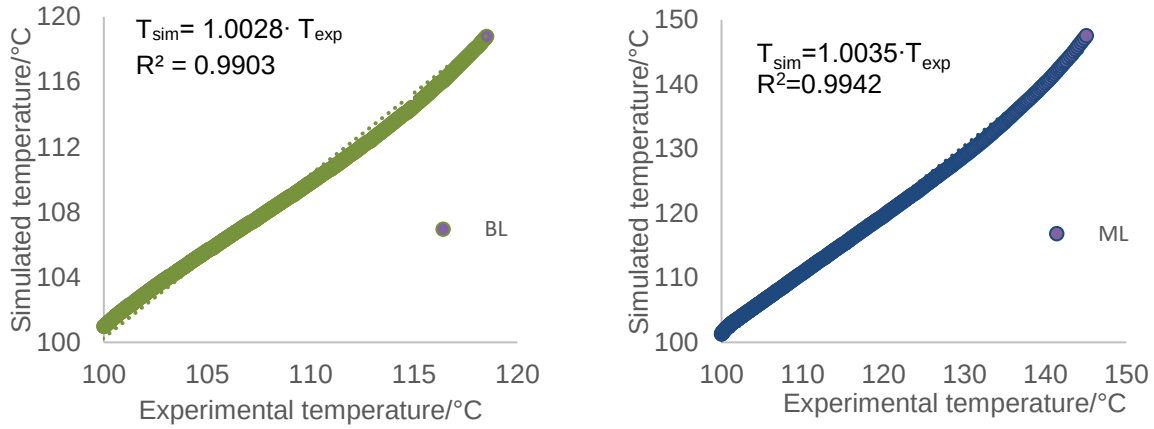

410

411 Fig. 7 - Overall parity plots of experimental temperature versus simulated temperatures for BL

412 and ML systems.

413

One can notice that the kinetics of ML hydrogenation is faster than BL hydrogenation, as it was demonstrated in previous articles (Negahdar et al., 2017; Wang et al., 2019). Based on this model, it is possible to estimate different thermal risk parameters under the same operating conditions as described in Table 9.

Table 9. Thermal risk parameters for the hydrogenation of ML and BL.

	T_{D24} (°C)	T_{D8} (°C)	TMR_{ad}(100°C) (hrs)	ΔT_{ad} (°C)
Hydrogenation of ML	49	62	0.55	66
Hydrogenation of BL	60	74	1.20	47

By using the criteria defined in the article by Wang et al. (2018), both reaction systems present a medium thermal risk with the operating conditions of Table 2. Even if for BL system, the TMR_{ad}(100°C) value gives a probable risk and ΔT_{ad} value gives a medium severity, one should keep in mind that this reaction system is under hydrogen pressure.

Further information can be provided by calculating the values of T_{D24} and $T_{D8.}$ These parameters represent the initial temperature under adiabatic mode to reach the fastest temperature rate in 24 hours and 8 hours. One should notice that the values of these parameters are lower than 100°C. The classical temperature for this reaction system can be up to 160°C under isothermal conditions. Hence, safety barriers, such as an additional cooling system, must be added in the case of thermal runaway.

4. CONCLUSIONS

In this study, thermal risk assessment for the production of γ-valerolactone (GVL) from the hydrogenation of methyl levulinate (ML) and butyl levulinate (BL) over Ru/C was carried out. To achieve this goal, the reaction enthalpies were measured, and kinetic models were developed based on experiments performed under adiabatic conditions. For that, two types of calorimeters were used: Mettler Toledo RC1 and Setaram Tian-Calvet C80.

Hydrogenation of alkyl levulinates over Ru/C is a two-step reaction: hydrogenation and cyclization. It was experimentally found that the overall reaction is exothermic. The hydrogenation reaction enthalpy was calculated to be -53.25 kJ/mol for the ML hydrogenation and -38.66 kJ/mol for the BL hydrogenation. These values confirm the exothermic behavior of the first reaction step. The cyclization reaction enthalpy was measured to be +7 kJ/mol for the ML system and +6.5 kJ/mol for the BL system. These values show that this second reaction step is endothermic, and it is negligible compared to the hydrogenation step.

Adiabatic experiments in RC1 calorimeter were performed with the following operating conditions: initial substrate concentration of ca. 4.5 mol/L, dry basis catalyst loading of 5.4×10^{-3} kg/L, and initial reaction temperature of 100°C. It was found that the thermal risk for both systems can be considered as a medium for such operating conditions based on TMR_{ad} and ΔT_{ad}. Safety barriers must be implemented for such a reaction system to decrease the risk of thermal runaway. A further investigation is to evaluate the optimum operating conditions to find a compromise between safety and productivity.

ACKNOWLEDGEMENTS

This study has been done in the framework of Task 2: “Green process: 2nd generation of biomass” of AMED project. The authors thank the AMED project. The AMED project has been funded with the support from the European Union with the European Regional Development Fund (ERDF) and from the Regional Council of Normandie. The China Scholarship Council: Cooperation Program with the UTs and INSAs (France) is thanked by the authors. The authors also thank the PHC program Proteus “Process intensification in the production of 2nd generation platform molecules” (41657WB). The authors thank Jean-Pierre Hébert for his huge help for the experimental part with the Mettler Toledo RC1.

NOMENCLATURE

C_P	Specific heat-capacity [J/(kg.K)]
Ea	Activation energy [J/mol]
ΔH_R	Reaction enthalpy [J/mol]
k	Rate constant
V_{liq}	Volume of liquid [L]
m_{insert}	Insert mass [kg]
P	Pressure [bar]
R	Gas constant [J/(K.mol)]
R^2	Coefficient of determination [%]
ΔT_{ad}	Adiabatic temperature rise [°C]
T_R	Temperature of the reaction mixture [°C]
T_{Ref}	Reference temperature [°C]
R_i	reaction rate *i* [mol/(L.s)]
w_i	weight percent
y_i	experimental observable
$\bar{y}$	mean value of the experimental observables
$\hat{y}_i$	observable simulated by the model

Greek letters

ω	Objective function
$\omega_{Cat.}$	catalyst loading [kg/L]

468 **Subscripts and superscripts**

Ref	reference
*	interfacial value

469

470 **Abbreviations**

BL	butyl levulinate
BHP	n-butyl 4-hydroxypentanoate
GVL	γ-valerolactone
ML	methyl levulinate
MHP	methyl 4-hydroxypentanoate
ROH	co-product of the second reaction (methanol or butanol)
TMR_{ad}	Time-to-maximum rate under adiabatic conditions at T_P [hrs]

471

472

473

REFERENCES

Al-Naji, M., Puértolas, B., Kumru, B., Cruz, D., Bäumel, M., Schmidt, B.V.K.J., Tarakina, N.V., Pérez-Ramírez, J., 2019. Sustainable continuous flow valorization of γ-valerolactone with trioxane to α-methylene-γ-valerolactone over basic beta zeolites. ChemSusChem 12, 2628–2636. https://doi.org/10.1002/cssc.201900418

Alonso, D.M., Wettstein, S.G., Mellmer, M.A., Gurbuz, E.I., Dumesic, J.A., 2012. Integrated conversion of hemicellulose and cellulose from lignocellulosic biomass. Energy Environ. Sci. 6, 76–80. https://doi.org/10.1039/C2EE23617F

Al-Shaal, M.G., Calin, M., Delidovich, I., Palkovits, R., 2016. Microwave-assisted reduction of levulinic acid with alcohols producing γ-valerolactone in the presence of a Ru/C catalyst. Catal. Commun. 75, 65–68. https://doi.org/10.1016/j.catcom.2015.12.001

An, R., Xu, G., Chang, C., Bai, J., Fang, S., 2017. Efficient one-pot synthesis of n-butyl levulinate from carbohydrates catalyzed by $Fe_2(SO_4)_3$. J. Energy Chem. 26, 556–563. https://doi.org/10.1016/j.jechem.2016.11.015

Bollyn, M., 2006. DMSO can be more than a solvent: thermal analysis of its chemical interactions with certain chemicals at different process stages. Org. Process Res. Dev. 10, 1299–1312. https://doi.org/10.1021/op060158p

Bond, J.Q., Alonso, D.M., Wang, D., West, R.M., Dumesic, J.A., 2010. Integrated catalytic conversion of γ-valerolactone to liquid alkenes for transportation fuels. Science 327, 1110–1114. https://doi.org/10.1126/science.1184362

Borregaard, 2019. Capacity increase for bio-based vanillin. https://www.borregaard.com/News/Capacity-increase-for-bio-based-vanillin (accessed 3 July 2020).

Bourne, R.A., Stevens, J.G., Ke, J., Poliakoff, M., 2007. Maximising opportunities in supercritical chemistry: the continuous conversion of levulinic acid to γ-valerolactone in CO_2. Chem.

Commun. 4632–4634. https://doi.org/10.1039/B708754C

Bozell, J.J., Moens, L., Elliott, D.C., Wang, Y., Neuenscwander, G.G., Fitzpatrick, S.W., Bilski, R.J., Jarnefeld, J.L., 2000. Production of levulinic acid and use as a platform chemical for derived products. Resour. Conserv. Recy. 28, 227–239. https://doi.org/10.1016/S0921-3449(99)00047-6

Brown, D.B., Ironside, M.D., Shaw, S.M., 2016. Safety notables: Information from the literature. Org. Process Res. Dev. 20, 575–582. https://doi.org/10.1021/acs.oprd.6b00013

Budzianowski, W.M., Postawa, K., 2016. Total Chain Integration of sustainable biorefinery systems. Appl. Energy 184, 1432–1446. https://doi.org/10.1016/j.apenergy.2016.06.050

Casson Moreno, V., Cozzani, V., 2015. Major accident hazard in bioenergy production. J. Loss Prevent. Proc. 35, 135–144. https://doi.org/10.1016/j.jlp.2015.04.004

Casson Moreno, V., Garbetti, A.L., Leveneur, S., Antonioni, G., 2019. A consequences-based approach for the selection of relevant accident scenarios in emerging technologies. Saf. Sci. 112, 142–151. https://doi.org/10.1016/j.ssci.2018.10.024

Casson Moreno, V., Papasidero, S., Scarponi, G.E., Guglielmi, D., Cozzani, V., 2016. Analysis of accidents in biogas production and upgrading. Renew. Energy 96, 1127–1134. https://doi.org/10.1016/j.renene.2015.10.017

Chandel, A.K., Garlapati, V.K., Kumar, S.P.J., Hans, M., Singh, A.K., Kumar, S., n.d. The role of renewable chemicals and biofuels in building a bioeconomy. Biofuel Bioprod. Biorefin. n/a. https://doi.org/10.1002/bbb.2104

Chew, A.K., Walker, T.W., Shen, Z., Demir, B., Witteman, L., Euclide, J., Huber, G.W., Dumesic, J.A., Van Lehn, R.C., 2020. Effect of mixed-solvent environments on the selectivity of acid-catalyzed dehydration reactions. ACS Catal. 10, 1679–1691. https://doi.org/10.1021/acscatal.9b03460

Chi, J.-H., Wu, S.-H., Shu, C.-M., 2009. Thermal explosion analysis of methyl ethyl ketone peroxide by non-isothermal and isothermal calorimetric applications. J. Hazard. Mater. 171,

524 1145–1149. https://doi.org/10.1016/j.jhazmat.2009.06.125
525 Dakkoune, A., Vernières-Hassimi, L., Leveneur, S., Lefebvre, D., Estel, L., 2018. Risk analysis
526 of French chemical industry. Saf. Sci. 105, 77–85. https://doi.org/10.1016/j.ssci.2018.02.003
527 Delhaye, L., Stevens, C., Merschaert, A., Delbeke, P., Briône, W., Tilstam, U., Borghese, A.,
528 Geldhof, G., Diker, K., Dubois, A., Barberis, M., Casarubios, L., 2007. Development of a scalable
529 process for the synthesis of trans-2-methylcyclopropanecarboxylic acid. Org. Process Res. Dev.
530 11, 1104–1111. https://doi.org/10.1021/op600275g
531 di Bitonto, L., Antonopoulou, G., Braguglia, C., Campanale, C., Gallipoli, A., Lyberatos, G.,
532 Ntaikou, I., Pastore, C., 2018. Lewis-Brønsted acid catalysed ethanolysis of the organic fraction
533 of municipal solid waste for efficient production of biofuels. Bioresour. Technol. 266, 297–305.
534 https://doi.org/10.1016/j.biortech.2018.06.110
535 Ding, D., Xi, J., Wang, J., Liu, X., Lu, G., Wang, Y., 2015. Production of methyl levulinate from
536 cellulose: selectivity and mechanism study. Green Chem. 17, 4037–4044.
537 https://doi.org/10.1039/C5GC00440C
538 Dockerty, T., Appleton, K., Lovett, A., 2012. Public opinion on energy crops in the landscape:
539 considerations for the expansion of renewable energy from biomass. J. Environ. Plan. Manag. 55,
540 1134–1158. https://doi.org/10.1080/09640568.2011.636966
541 Dong, Z., Chen, L., Ma, Y., Peng, H., Chen, W., 2018. Adiabatic correction for the esterification
542 of acetic anhydride by methanol via accurate kinetics. Chin. J. Chem. Eng. 26, 1954–1959.
543 https://doi.org/10.1016/j.cjche.2017.10.005
544 Dutta, S., Yu, I.K.M., Tsang, D.C.W., Ng, Y.H., Ok, Y.S., Sherwood, J., Clark, J.H., 2019. Green
545 synthesis of gamma-valerolactone (GVL) through hydrogenation of biomass-derived levulinic
546 acid using non-noble metal catalysts: A critical review. Chem. Eng. J. 372, 992–1006.
547 https://doi.org/10.1016/j.cej.2019.04.199
548 Feng, X., Tian, Y., Xiao, L., Wu, W., 2020. Fe–Mo_2C: A magnetically recoverable catalyst for

549 hydrogenation of ethyl levulinate into γ-valerolactone. Catal Lett.
550 https://doi.org/10.1007/s10562-020-03124-z
551 Gallezot, P., 2012. Conversion of biomass to selected chemical products. Chem. Soc. Rev. 41,
552 1538–1558. https://doi.org/10.1039/C1CS15147A
553 Gigante, L., Lunghi, A., Martinelli, S., Cardillo, P., Picello, L., Bortolaso, R., Galvagni, M., Rota,
554 R., 2003. Calorimetric approach and simulation for scale-up of a Friedel−Crafts reaction. Org.
555 Process Res. Dev. 7, 1079–1082. https://doi.org/10.1021/op030043a
556 Girgis, M.J., Kiss, K., Ziltener, C.A., Prashad, M., Har, D., Yoskowitz, R.S., Basso, B., Repic,
557 O., Blacklock, T.J., Landau, R.N., 1997. Kinetic and calorimetric considerations in the scale-up
558 of the catalytic reduction of a substituted nitrobenzene. Org. Process Res. Dev. 1, 339–349.
559 https://doi.org/10.1021/op970015q
560 Golikova, A., Tsvetov, N., Samarov, A., Toikka, M., Zvereva, I., Trofimova, M., Toikka, A.,
561 2020. Excess enthalpies and heat of esterification reaction in ethanol + acetic acid + ethyl
562 acetate + water system at 313.15 K. J. Therm. Anal. Calorim. 139, 1301–1307.
563 https://doi.org/10.1007/s10973-019-08488-y
564 GranBio, 2014. GranBio begins producing second-generation ethanol. http://news.bio-
565 based.eu/granbio-begins-producing-second-generation-ethanol/ (accessed 3 July 2020).
566 Haario, H., 2001. MODEST-User's Guide, in: Profmath Oy, Helsinki.
567 Hayes, D. J., Fitzpatrick, S., Hayes, M. H. B, Ross, J. R. H., 2005. The Biofine Process –
568 Production of Levulinic Acid, Furfural, and Formic Acid from Lignocellulosic Feedstocks, in
569 Biorefineries-Industrial Processes and Products: Status Quo and Future Directions, in: Kamm, B.,
570 Gruber, P. R., Kamm, M. (Eds.), Wiley-VCH Verlag GmbH, Weinheim.
571 Hoffmann, W., Kang, Y., Mitchell, J.C., Snowden, M.J., 2007. Kinetic data by nonisothermal
572 reaction calorimetry: a model-assisted calorimetric evaluation. Org. Process Res. Dev. 11, 25–
573 29. https://doi.org/10.1021/op060144j

574 Horváth, I.T., Mehdi, H., Fábos, V., Boda, L., Mika, L.T., 2008. γ-valerolactone—a sustainable
575 liquid for energy and carbon-based chemicals. Green Chem. 10, 238–242.
576 https://doi.org/10.1039/B712863K
577 Huber, G.W., Iborra, S., Corma, A., 2006. Synthesis of transportation fuels from biomass:
578 chemistry, catalysts, and engineering. Chem. Rev. 106, 4044–4098.
579 https://doi.org/10.1021/cr068360d
580 Jhu, C.-Y., Wang, Y.-W., Wen, C.-Y., Shu, C.-M., 2012. Thermal runaway potential of $LiCoO_2$
581 and $Li(Ni1/3Co1/3Mn1/3)O_2$ batteries determined with adiabatic calorimetry methodology.
582 Applied Energy, Clean Energy for Future Generations 100, 127–131.
583 https://doi.org/10.1016/j.apenergy.2012.05.064
584 Kortsch, T., Hildebrand, J., Schweizer-Ries, P., 2015. Acceptance of biomass plants – Results of
585 a longitudinal study in the bioenergy-region Altmark. Renew. Energy 83, 690–697.
586 https://doi.org/10.1016/j.renene.2015.04.059
587 Leveneur, S., 2017. Thermal safety assessment through the concept of structure–reactivity:
588 application to vegetable oil valorization. Org. Process Res. Dev. 21, 543–550.
589 https://doi.org/10.1021/acs.oprd.6b00405
590 Leveneur, S., Pinchard, M., Rimbault, A., Safdari Shadloo, M., Meyer, T., 2018. Parameters
591 affecting thermal risk through a kinetic model under adiabatic condition: Application to liquid-
592 liquid reaction system. Thermochim. Acta 666, 10–17. https://doi.org/10.1016/j.tca.2018.05.024
593 Leveneur, S., Vernieres-Hassimi, L., Salmi, T., 2016. Mass & energy balances coupling in
594 chemical reactors for a better understanding of thermal safety. Educ. Chem. Eng. 16, 17–28.
595 https://doi.org/10.1016/j.ece.2016.06.002
596 Li, F., Li, Z., France, L.J., Mu, J., Song, C., Chen, Y., Jiang, L., Long, J., Li, X., 2018. Highly
597 efficient transfer hydrogenation of levulinate esters to γ-valerolactone over basic zirconium
598 carbonate. Ind. Eng. Chem. Res. 57, 10126–10136. https://doi.org/10.1021/acs.iecr.8b00712

Lin, H., Chen, J., Zhao, Y., Wang, S., 2017. Conversion of C5 carbohydrates into furfural catalyzed by so3h-functionalized ionic liquid in renewable γ-valerolactone. Energ. Fuels 31, 3929–3934. https://doi.org/10.1021/acs.energyfuels.6b01975

Liu, C., Wei, M., Wang, J., Xu, J., Jiang, J., Wang, K., 2020. Facile directional conversion of cellulose and bamboo meal wastes over low-cost sulfate and polar aprotic solvent. ACS Sustainable Chem. Eng. 8, 5776–5786. https://doi.org/10.1021/acssuschemeng.0c01280

Liu, S.H., Hou, H.Y., Chen, J.W., Weng, S.Y., Lin, Y.C., Shu, C.M., 2013. Effects of thermal runaway hazard for three organic peroxides conducted by acids and alkalines with DSC, VSP2, and TAM III. Thermochim. Acta 566, 226–232. https://doi.org/10.1016/j.tca.2013.05.029

Lunghi, A., Alós, M.A., Gigante, L., Feixas, J., Sironi, E., Feliu, J.A., Cardillo, P., 2002. Identification of the decomposition products in an industrial nitration process under thermal runaway conditions. Org. Process Res. Dev. 6, 926–932. https://doi.org/10.1021/op0255884

Luo, W., Deka, U., Beale, A.M., van Eck, E.R.H., Bruijnincx, P.C.A., Weckhuysen, B.M., 2013. Ruthenium-catalyzed hydrogenation of levulinic acid: Influence of the support and solvent on catalyst selectivity and stability. J. Catal. 301, 175–186. https://doi.org/10.1016/j.jcat.2013.02.003

Luterbacher, J.S., Rand, J.M., Alonso, D.M., Han, J., Youngquist, J.T., Maravelias, C.T., Pfleger, B.F., Dumesic, J.A., 2014. Nonenzymatic sugar production from biomass using biomass-derived γ-valerolactone. Science 343, 277–280. https://doi.org/10.1126/science.1246748

Maestri, F., Re Dionigi, L., Rota, R., Gigante, L., Lunghi, A., Cardillo, P., 2006. Safe and productive operation of homogeneous semibatch reactors. II. The nitration of N-(2-Phenoxyphenyl) methane sulfonamide. Ind. Eng. Chem. Res. 45, 8014–8023. https://doi.org/10.1021/ie060262v

Makhubela, B.C.E., Darkwa, J., 2018. The role of noble metal catalysts in conversion of biomass and bio-derived intermediates to fuels and chemicals. Johnson Matthey Technology Review 62,

4–31. https://doi.org/10.1595/205651317X696261

Marco, E., Cuartielles, S., Peña, J.A., Santamaria, J., 2000. Simulation of the decomposition of di-cumyl peroxide in an ARSST unit. Thermochim. Acta 362, 49–58. https://doi.org/10.1016/S0040-6031(00)00587-6

Mellmer, M.A., Alonso, D.M., Luterbacher, J.S., Gallo, J.M.R., Dumesic, J.A., 2014. Effects of γ-valerolactone in hydrolysis of lignocellulosic biomass to monosaccharides. Green Chem. 16, 4659–4662. https://doi.org/10.1039/C4GC01768D

Negahdar, L., Al-Shaal, M.G., Holzhäuser, F.J., Palkovits, R., 2017. Kinetic analysis of the catalytic hydrogenation of alkyl levulinates to γ-valerolactone. Chem. Eng. Sci. 158, 545–551. https://doi.org/10.1016/j.ces.2016.11.007

Peng, L., Lin, L., Zhang, J., Shi, J., Liu, S., 2011. Solid acid catalyzed glucose conversion to ethyl levulinate. Appl. Catal. A-Gen. 397, 259–265. https://doi.org/10.1016/j.apcata.2011.03.008

Pérez-Sena, W.Y., Salmi, T., Estel, L., Leveneur, S., 2020. Thermal risk assessment for the epoxidation of linseed oil by classical Prisleschajew epoxidation and by direct epoxidation by H_2O_2 on alumina. J. Therm. Anal. Calorim. 140, 673–684. https://doi.org/10.1007/s10973-019-08894-2

Piskun, A.S., van de Bovenkamp, H.H., Rasrendra, C.B., Winkelman, J.G.M., Heeres, H.J., 2016. Kinetic modeling of levulinic acid hydrogenation to γ-valerolactone in water using a carbon supported Ru catalyst. Appl. Catal. A-Gen. 525, 158–167. https://doi.org/10.1016/j.apcata.2016.06.033

Pokorný, V., Štejfa, V., Fulem, M., Červinka, C., Růžička, K., 2017. Vapor pressures and thermophysical properties of ethylene carbonate, propylene carbonate, γ-valerolactone, and γ-butyrolactone. J. Chem. Eng. Data 62, 4174–4186. https://doi.org/10.1021/acs.jced.7b00578

Protsenko, I.I., Nikoshvili, L.Zh., Matveeva, V.G., Sulman, E.M., 2020. Kinetic modelling of levulinic acid hydrogenation over ru-containing polymeric catalyst. Top. Catal. 63, 243–253.

https://doi.org/10.1007/s11244-020-01223-0

Pulidindi, I.N., Kim, T.H., 2018. Conversion of levulinic acid from various herbaceous biomass species using hydrochloric acid and effects of particle size and delignification. Energies 11, 621. https://doi.org/10.3390/en11030621

Qi, L., Horváth, I.T., 2012. Catalytic conversion of fructose to γ-valerolactone in γ-valerolactone. ACS Catal. 2, 2247–2249. https://doi.org/10.1021/cs300428f

Rodenas, Y., Mariscal, R., Fierro, J.L.G., Alonso, D.M., Dumesic, J.A., Granados, M.L., 2018. Improving the production of maleic acid from biomass: TS-1 catalysed aqueous phase oxidation of furfural in the presence of γ-valerolactone. Green Chem. 20, 2845–2856. https://doi.org/10.1039/C8GC00857D

Saha, N., Al-Muhannadi, R., Al-Mohannadi, A., Véchot, L.N., Castier, M., 2018. Is it the time to say bye to the ϕ-factor? Process Saf. Environ. 113, 193–203. https://doi.org/10.1016/j.psep.2017.10.009

Sempere, J., Nomen, R., Serra, R., Cardillo, P., 1997. Thermal hazard assessment using closed-cell adiabatic calorimetry. J. Loss Prevent. Proc. 10, 55–62. https://doi.org/10.1016/S0950-4230(96)00035-6

Sener, C., Motagamwala, A.H., Alonso, D.M., Dumesic, J.A., 2018. Enhanced furfural yields from xylose dehydration in the γ-valerolactone/water solvent system at elevated temperatures. ChemSusChem 11, 2321–2331. https://doi.org/10.1002/cssc.201800730

Serrano-Ruiz, J.C., Wang, D., Dumesic, J.A., 2010. Catalytic upgrading of levulinic acid to 5-nonanone. Green Chem. 12, 574–577. https://doi.org/10.1039/B923907C

Shen, Y., Zhu, W., Papadaki, M., Mannan, M.S., Mashuga, C.V., Cheng, Z., 2019. Thermal decomposition of solid benzoyl peroxide using advanced reactive system screening tool: effect of concentration, confinement and selected acids and bases. J. Loss Prevent. Proc. 60, 28–34. https://doi.org/10.1016/j.jlp.2019.04.001

Sikorska, D., Macegoniuk, S., Łaszkiewicz, E., Sikorski, P., 2020. Energy crops in urban parks as a promising alternative to traditional lawns – Perceptions and a cost-benefit analysis. Urban For. Urban Gree. 49, 126579. https://doi.org/10.1016/j.ufug.2019.126579

Singh, J., 1993. Reliable scale-up of thermal hazards data using the PHI-TEC II calorimeter. Thermochim. Acta 226, 211–220. https://doi.org/10.1016/0040-6031(93)80222-V

Soland, M., Steimer, N., Walter, G., 2013. Local acceptance of existing biogas plants in Switzerland. Energy Policy 61, 802–810. https://doi.org/10.1016/j.enpol.2013.06.111

Stoessel, F., 2008. Thermal safety of chemical processes, in:Wiley-VCH Verlag GmbH & Co, Weinheim.

Sun, Y., Ni, L., Papadaki, M., Zhu, W., Jiang, J., Mashuga, C., Wilhite, B., Mannan, M.S., 2019. Process hazard evaluation for catalytic oxidation of 2-octanol with hydrogen peroxide using calorimetry techniques. Chem. Eng. J. 378, 122018. https://doi.org/10.1016/j.cej.2019.122018

Tang, W., Sarvestani, M., Wei, X., Nummy, L.J., Patel, N., Narayanan, B., Byrne, D., Lee, H., Yee, N.K., Senanayake, C.H., 2009. Formation of 2-trifluoromethylphenyl grignard reagent via magnesium−halogen exchange: Process safety evaluation and concentration effect. Org. Process Res. Dev. 13, 1426–1430. https://doi.org/10.1021/op900040y

Tang, X., Chen, H., Hu, L., Hao, W., Sun, Y., Zeng, X., Lin, L., Liu, S., 2014. Conversion of biomass to γ-valerolactone by catalytic transfer hydrogenation of ethyl levulinate over metal hydroxides. Appl. Catal. B: Environ. 147, 827–834. https://doi.org/10.1016/j.apcatb.2013.10.021

Tanwongwan, W., Eiad-ua, A., Kraithong, W., Viriya-empikul, N., Suttisintong, K., Klamchuen, A., Kasamechonchung, P., Khemthong, P., Faungnawakij, K., Kuboon, S., 2019. Simultaneous activation of copper mixed metal oxide catalysts in alcohols for gamma-valerolactone production from methyl levulinate. Appl. Catal. A: Gen. 579, 91–98. https://doi.org/10.1016/j.apcata.2019.04.011

Tseng, J.-M., Lin, J.-Z., Lee, C.-C., Lin, C.-P., 2012. Prediction of TMCH thermal hazard with

699 various calorimetric tests by green thermal analysis technology. AIChE J. 58, 3792–3798.
700 https://doi.org/10.1002/aic.13745
701 Tukacs, J.M., Fridrich, B., Dibó, G., Székely, E., Mika, L.T., 2015. Direct asymmetric reduction
702 of levulinic acid to gamma-valerolactone: synthesis of a chiral platform molecule. Green Chem.
703 17, 5189–5195. https://doi.org/10.1039/C5GC01099C
704 Upham, P., Shackley, S., 2007. Local public opinion of a proposed 21.5MW(e) biomass gasifier
705 in Devon: Questionnaire survey results. Biomass Bioenerg. 31, 433–441.
706 https://doi.org/10.1016/j.biombioe.2007.01.017
707 Valdes, O.R., Moreno, V.C., Waldram, S., Véchot, L., Mannan, M.S., 2016. Runaway
708 decomposition of dicumyl peroxide by open cell adiabatic testing at different initial conditions.
709 Process Saf. Environ. 102, 251–262. https://doi.org/10.1016/j.psep.2016.03.021
710 Veedhi, S., Mishra, V., Kulkarni, S., Gorthi, R., 2014. Incident investigation on thermal instability
711 of an intermediate using adiabatic calorimeter. J. Therm. Anal. Calorim. 115, 909–914.
712 https://doi.org/10.1007/s10973-013-3327-5
713 Veedhi, S., Sawant, A., 2013. Designing a safer process for the reaction of TFA with sodium
714 borohydride in THF by calorimetric technique. J. Therm. Anal. Calorim. 111, 1093–1097.
715 https://doi.org/10.1007/s10973-012-2514-0
716 Vernières-Hassimi, L., Dakkoune, A., Abdelouahed, L., Estel, L., Leveneur, S., 2017. Zero-order
717 versus intrinsic kinetics for the determination of the time to maximum rate under adiabatic
718 conditions (TMR_{ad}): Application to the decomposition of hydrogen peroxide. Ind. Eng. Chem.
719 Res. 56, 13040–13049. https://doi.org/10.1021/acs.iecr.7b01291
720 Wang, J., Mannan, M.S., Wilhite, B.A., 2020. Integrated thermodynamic and kinetic model of
721 homogeneous catalytic N-oxidation processes. AIChE J. 66, e16875.
722 https://doi.org/10.1002/aic.16875
723 Wang, Y., Cipolletta, M., Vernières-Hassimi, L., Casson-Moreno, V., Leveneur, S., 2019.

724 Application of the concept of Linear Free Energy Relationships to the hydrogenation of levulinic
725 acid and its corresponding esters. Chem. Eng. J. 374, 822–831.
726 https://doi.org/10.1016/j.cej.2019.05.218
727 Wang, Y., Vernières-Hassimi, L., Casson-Moreno, V., Hébert, J.-P., Leveneur, S., 2018. Thermal
728 risk assessment of levulinic acid hydrogenation to γ-valerolactone. Org. Process Res. Dev. 22,
729 1092–1100. https://doi.org/10.1021/acs.oprd.8b00122
730 Wang, Z., Cao, D., Xu, Z., Wang, J., Chen, L., 2020. Thermal safety study on the synthesis of
731 HMX by nitrourea method. Process Saf. Environ. 137, 282–288.
732 https://doi.org/10.1016/j.psep.2020.02.013
733 Wettstein, S.G., Alonso, D.M., Chong, Y., Dumesic, J.A., 2012. Production of levulinic acid and
734 gamma-valerolactone (GVL) from cellulose using GVL as a solvent in biphasic systems. Energy
735 Environ. Sci. 5, 8199–8203. https://doi.org/10.1039/C2EE22111J
736 Wojciechowska, J., Jędrzejczyk, M., Grams, J., Keller, N., Ruppert, A.M., 2019. Enhanced
737 production of γ-valerolactone with an internal source of hydrogen on Ca-modified TiO_2 supported
738 Ru catalysts. ChemSusChem 12, 639–650. https://doi.org/10.1002/cssc.201801974
739 Wong, J.T., 2012. Technological, commercial, organizational, and social uncertainties of a novel
740 process for vanillin production from lignin. https://core.ac.uk/download/pdf/56377175.pdf
741 (accessed 3 July 2020)
742 Wright, W.R.H., Palkovits, R., 2012. Development of heterogeneous catalysts for the conversion
743 of levulinic acid to γ-valerolactone. ChemSusChem 5, 1657–1667.
744 https://doi.org/10.1002/cssc.201200111
745 Wu, S.-H., Wang, Y.-W., Wu, T.-C., Hu, W.-N., Shu, C.-M., 2008. Evaluation of thermal hazards
746 for dicumyl peroxide by DSC and VSP2. J. Therm. Anal. Calorim. 93, 189–194.
747 https://doi.org/10.1007/s10973-007-8874-1
748 Wu, X., Fu, J., Lu, X., 2012. One-pot preparation of methyl levulinate from catalytic alcoholysis

749 of cellulose in near-critical methanol. Carbohydr. Res. 358, 37–39.
750 https://doi.org/10.1016/j.carres.2012.07.002
751 Yan, K., Yang, Y., Chai, J., Lu, Y., 2015. Catalytic reactions of gamma-valerolactone: A platform
752 to fuels and value-added chemicals. Appl. Catal. B: Environ. 179, 292–304.
753 https://doi.org/10.1016/j.apcatb.2015.04.030
754 Zhang, Y., Chung, Y.-H., Liu, S.-H., Shu, C.-M., Jiang, J.-C., 2017. Analysis of thermal hazards
755 of O,O-dimethylphosphoramidothioate by DSC, TG, VSP2, and GC/MS. Thermochim. Acta 652,
756 69–76. https://doi.org/10.1016/j.tca.2017.03.014
757 Zheng, J.L., Wärnå, J., Salmi, T., Burel, F., Taouk, B., Leveneur, S., 2016. Kinetic modeling
758 strategy for an exothermic multiphase reactor system: Application to vegetable oils epoxidation
759 using Prileschajew method. AIChE J. 62, 726–741. https://doi.org/10.1002/aic.15037
760 Zoellner, J., Schweizer-Ries, P., Wemheuer, C., 2008. Public acceptance of renewable energies:
761 Results from case studies in Germany. Energy Policy, Transition towards Sustainable Energy
762 Systems 36, 4136–4141. https://doi.org/10.1016/j.enpol.2008.06.026
763